ChemPhotoChem

Research Article
doi.org/10.1002/cptc.202400149

Chemistry Europe
European Chemical Societies Publishing

www.chemphotochem.org

Aqueous Synthesis of Green Fluorescence Non-Conjugated Polymer Nanoparticles by *In Situ* Formation of Poly-Ionic Complexes

Ho Chun Wong,[a] Leong Ting Ng,[a] Ying Kau Lam,[a] and Pei Li*[a]

We present a novel method for synthesizing water-based non-conjugated polymer nanoparticles that possess green fluorescence. This synthesis involves the crosslinking of polyethyleneimine (PEI) with glutaraldehyde (GA), followed by *in situ* polymerization of an acrylic acid-based monomer. The nanoparticles are formed through self-assembly driven by *in situ* electrostatic complexation, resulting in unique photoluminescence properties. This process involves the negatively charged polymer, formed via graft and homo-polymerization, interacting with the pre-existing positively charged PEI. The nanoparticles consist solely of heteroatomic bonds like C–O, C–N, C=O, and C=N. The restriction of vibrational and rotational relaxation of these bonds within the nanoscale poly-ionic complex enhances their photoluminescence properties. For example, glutaraldehyde-crosslinked polyethyleneimine/poly(methacrylic acid) (gPEI/PMAA) nanoparticles produced by this method demonstrate outstanding properties including a narrow size distribution with an average diameter of 35 nm, excitation-dependent fluorescence with a green emission peak at 527 nm when excited at 480 nm, and a high quantum yield of up to 23.6% (± 1.2%). The green fluorescence property of the nanoparticles can be used in the generation of white LED light through incorporating them with silicone and coating them onto a blue light LED chip. This study represents a significant improvement in the fluorescence properties of PEI-based materials and opens up new possibilities for their applications in various fields.

1. Introduction

Over the past decades, conventional organic fluorescent materials containing conjugated aromatic systems such as fluorescent dyes, fluorescent proteins, or conjugated polymers have been extensively used in fields such as textile dyeing,[1] lighting,[2] biological imaging,[3] medical diagnosis,[4] anti-counterfeiting,[5] and constructing topological microsphere clusters.[6] However, these materials suffer from the quenching effect caused by aggregation when they are in solid or aggregated states. This effect, which arises due to the rigid π-conjugated structures of these materials, has limited their practical applications.[7] To overcome this limitation, aggregation-induced emission (AIE) luminogenic molecules have emerged as an alternative to traditional organic dye molecules. AIE luminogens were first reported by Tang's group in 2001 and have received extensive attention due to their ability to emit light in the aggregated state.[8–9] Unlike conventional fluorescent materials, AIE luminogens exhibit enhanced emission when they aggregate, resulting in a phenomenon known as aggregation-induced emission (AIE).[10]

Fluorescent nanoparticles comprising non-conjugated polymers represent a novel class of photoluminescent nanomaterials that possess good water dispersibility, biocompatibility, stability, and low toxicity. These properties render them highly suitable for a wide range of applications, including bioimaging,[11,12] drug delivery,[13,14] chemical detection,[15–23] logic gates,[24] and temperature sensors.[20] In general, polymers containing heteroatoms of both single bonds (e.g. N–H, C–O, C–N, N–O) and double bonds (e.g. C=O, C=N, N=O) exhibit very weak fluorescence.[25] However, their photoluminescence (PL) can be significantly enhanced by immobilizing them through chemical or physical means to restrict their vibrational and rotational relaxation. One effective approach for immobilization is the utilization of crosslink-enhanced emission (CEE) effects, which encompass various mechanisms such as supramolecular-interaction CEE, ionic-bonding CEE, and confined-domain CEE.[26–27] Another strategy involves the clustering of electronic-rich functional groups, known as clustering-triggered emission (CTE).[28] By confining the sub-fluorophores to a smaller volume, a more efficient luminescence can be achieved via through-space conjugation (TSC), which is induced by a rigid conformation of chromophore clusters.[29] Using the concepts of CEE and CTE, non-conjugated fluorescence nanoparticles have been prepared from precursor polymers or monomers by means of polymerization,[11,15,16] crosslinking,[15,22,30] or self-assembly.[12,13,17]

Branched polyethyleneimine (PEI), a water-soluble polymer known for its highly positive charges, is derived from primary, secondary and tertiary amino groups. Polyethyleneimine (PEI), a water-soluble polymer known for its highly positive charges, is

[a] H. Chun Wong, L. Ting Ng, Y. Kau Lam, P. Li
Department of Applied Biology and Chemical Technology, The Hong Kong Polytechnic University, Hung Hom, Kowloon, Hong Kong, P. R. China
E-mail: pei.li@polyu.edu.hk

Supporting information for this article is available on the WWW under https://doi.org/10.1002/cptc.202400149

derived from primary amine ($-NH_2$) and secondary amine ($-NH-$) groups. These active amine groups enable easy modifications of PEI through various chemical reactions, and have led to the synthesis of diverse PEI-based materials for a wide range of applications such as sensing,[31] bioimaging,[32,33] gene delivery,[34–37] drug delivery,[38] antimicrobial films,[39,40] heavy metal ion removal,[41] and CO_2 adsorption.[42,43] The branched PEI molecules have been reported to exhibit very weak blue fluorescence with a quantum yield (QY) of less than 1%.[44] Several strategies for enhancing the fluorescence of PEI have been reported.[12,17,19–25,30] For example, Yang *et al.* crosslinked PEI with carbon tetrachloride (CTC) to result in a QY of 2.7% and a maximum emission at 475 nm when excited by 400 nm light.[25] In another study, Liu *et al.* modified PEI with boronic acid, leading to a QY of 8.7% and a maximum emission at 500 nm when excited by 380 nm light.[21] Han *et al.* described the synthesis of green emissive polymer dots by combining PEI with tetrakis(hydroxymethyl)phosphonium chloride (THPC).[23] The resulting polymer dots exhibited a high quantum yield (QY) of 25% with a maximum emission at 515 nm upon excitation by 400 nm light. However, these modified PEIs typically require high-energy light excitation in the range of 360 to 400 nm to achieve the highest emission intensity.

In this study, we introduce a novel method for producing polymer nanoparticles with green fluorescence. This process involves *in situ* electrostatic complexation between a negatively charged polymer, generated via free-radical polymerization, and pre-existing positively charged polyethyleneimine (PEI) to form poly-ionic complexes. The main advantage of using electrostatic interactions to restrict PEI motion, compared to crosslinking, is the minimal structural alteration, which preserves the original structure and properties. Moreover, electrostatic interactions can occur spontaneously during polymerization, eliminating the need for complex chemical reactions required for crosslinking. Furthermore, the nanoparticles formed through strong electrostatic interaction are much more compact than those created by crosslinking. This increased compactness may lead to red-shifted photoluminescence due to enhanced electronic delocalization.

Our approach involves a two-step reaction: First, crosslinking PEIwith glutaraldehyde (GA) in ethanol; Second, *in situ* polymerization of an acrylic acid-based monomer in an aqueous medium (Scheme 1). This process utilizes electrostatic complexation between a negatively charged polymer which was generated by the free-radical polymerization and a pre-existing positively charged PEI to form poly-ionic complexes. Among various nanoparticles synthesized, the glutaraldehyde-crosslinked PEI/poly(methacrylic acid) (gPEI/PMAA) nanoparticles demonstrated the most desirable characteristics, which included a high degree of monodispersity with an average diameter of 35 nm, excitation-dependent fluorescence, and a maximum emission wavelength of 527 nm when excited at 480 nm in an aqueous dispersion. The quantum yield of the gPEI/PMAA nanoparticles reached 23.6% (±1.2%). This finding is significant because conventionally modified PEIs typically require high-energy light excitation in the range of 360 to 400 nm to achieve the highest emission intensity, often resulting in blue fluorescence. Additionally, our study represents the first report on the synthesis of green fluorescent nanoparticles based on PEI using simultaneous *in situ* polymerization and electrostatic self-assembly to form poly-ionic complexes. Moreover, our polymerization method offers scal-

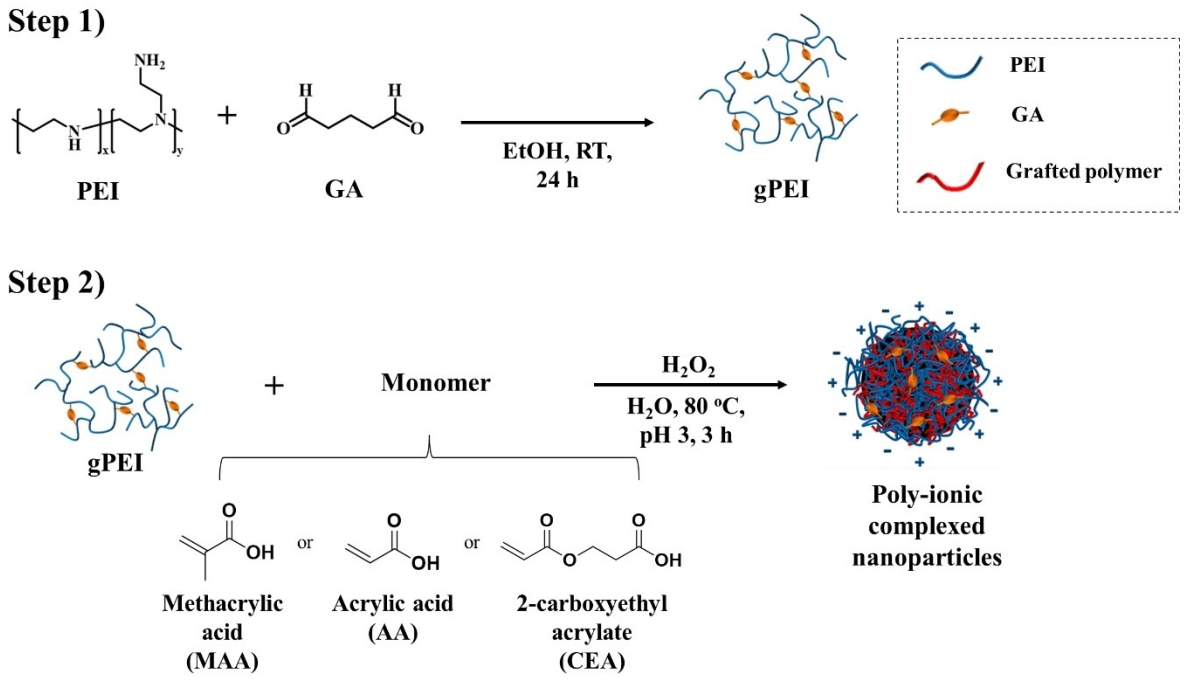

Scheme 1. A two-stage synthesis of green fluorescence nanoparticles: 1) PEI was crosslinked with 2 mol% of glutaraldehyde in an ethanol (EtOH) solution at room temperature for 24 hours. 2) In situ polymerization of an anionic monomer such as acrylic acid (AA), methacrylic acid (MAA), and 2-carboxyethyl acrylate (CEA) to form poly-ionic complexed nanoparticles.

ability for large-scale production, making it suitable for commercialization. For example, these water-dispersible, non-conjugated polymer nanoparticles with inherent photoluminescent properties have been utilized as green fluorescent fillers in white light-emitting diodes (WLEDs) that employ monochromatic blue LED chips as light sources.

2. Results and Discussion

2.1. Synthesis of gPEI/PMAA Poly-Ionic Complex Nanoparticles

The synthesis of green fluorescent nanoparticles, consisting of glutaraldehyde-crosslinked polyethyleneimine (gPEI) and poly(methacrylic acid) (PMAA), was carried out in two stages as illustrated in Scheme 1. In the first stage, PEI was crosslinked with glutaraldehyde (GA) in an ethanol solution at room temperature for 24 hours. PEI contains primary amine groups ($-NH_2$), while glutaraldehyde has two aldehyde groups ($-CHO$). These groups readily react to form imine bonds (C=N), known as Schiff bases. The imine bond formation between PEI's amine groups and GA's aldehyde groups resulted in the crosslinking of PEI chains, creating a network structure. After the reaction, ethanol was removed from the ethanol/water mixture, yielding an aqueous solution of gPEI, which appeared yellowish. The degree of crosslinking was controlled by adjusting the molar percentage of glutaraldehyde. It was found that using more than 3 mol% of GA caused precipitation, indicating excessive crosslinking. Therefore, 2 mol% GA was selected for optimal crosslinking without precipitation.

In the second stage, a water-soluble anionic monomer with carboxylic acid groups, such as acrylic acid (AA), methacrylic acid (MAA), or 2-carboxyethyl acrylate (CEA), underwent *in situ* free-radical polymerization. The reaction mechanism involves the interaction of the amine group from gPEI with a small amount of hydrogen peroxide in an aqueous medium, generating free radicals on the nitrogen atoms.[45] These radicals initiate the graft polymerization of a negatively charged, water-soluble monomer. Hydroxy radicals produced can either start the homo-polymerization of the monomer or abstract hydrogen from the gPEI backbone. The radicals on gPEI lead to graft copolymerization, forming negatively charged polyion chains on the PEI chain. Simultaneously, hydroxy radicals can independently polymerize the monomer, creating negatively charged homopolymers. These negatively charged polyion chains interact with positively charged gPEI, self-assembling into a neutral core with a 1:1 ratio of oppositely charged polymers. A shell of excess PEI chains surrounds the core, carrying a net positive charge. This charged corona stabilizes the nanoparticles by providing electrostatic repulsion, thus preventing aggregation.[46]

2.2. Effect of Reaction Conditions on the Synthesis of gPEI/PMAA Nanoparticles

The synthesis involves crosslinking PEI with glutaraldehyde to form gPEI, followed by *in situ* polymerization of an anionic monomer in the presence of gPEI. This process results in the formation of nanoparticles through electrostatic self-assembly. Careful control of reaction conditions and selection of monomers are essential for achieving the desired nanoparticle properties. The effects of reaction time and pH on the polymerization of MAA using a 1:2 weight ratio of gPEI to MAA were studied. Results shown in Figure S1 indicate that the monomer conversion gradually increased with increasing reaction time, reaching approximately 80% conversion after three hours. Further prolonging the reaction time from 3 to 4.5 hours did not significantly affect monomer conversion. Thus, the optimal reaction time for the synthesis of gPEI/PMAA nanoparticles was 3 hours.

Controlling the pH is essential for optimizing the formation and stability of poly-ionic complexes. At different pH levels, the ionization of acidic and basic groups on the polymers can change. For instance, acidic groups like carboxyl groups are more likely to be deprotonated and negatively charged at higher pH, while basic groups like amine groups tend to be protonated and positively charged at lower pH. The strength and nature of electrostatic interactions between oppositely charged polymers depend on their ionization states, and the stability of the poly-ionic complex can vary with pH. Additionally, pH can induce conformational changes in the polymers, affecting their interaction and assembly into complexes. Therefore, we investigated the influence of solution pH on the synthesis and photoluminescent properties of PEI-based nanoparticles at pH values of 1, 3, 5, 7, and 9 (Figure 1A). Results shown in Figure S2 indicated that nanoparticles synthesized at pH 3 and 5 exhibited narrow particle size distributions, whereas those synthesized at pH 1, 7, and 9 displayed multi-modal size distributions. The average particle sizes obtained at pH 3 and 5 were approximately 35 nm and 38 nm, respectively.

To examine the influence of pH on the photoluminescent properties of gPEI/PMAA nanoparticles, fluorescence intensities at pH 1, 3, 5, 7 and 9 were measured using a spectrofluorometer (Figure S3). Results summarized in Figure 1B revealed that gPEI/PMAA nanoparticles synthesized at pH 3 exhibited the highest fluorescence intensity, suggesting that this pH level is optimal for enhancing their photoluminescent properties. Furthermore, the maximum excitation and emission wavelengths were found to be at 480 nm and 527 nm, respectively, indicating the green fluorescence property of these nanoparticles. Therefore, the fluorescence intensity of the nanoparticles is sensitive to the pH during synthesis, indicating that pH plays a crucial role in determining their photoluminescent characteristics.

2.3. Effect of Monomer Structures

In the second stage of the synthesis, anionic monomers that contained carboxylic acid groups such as acrylic acid (AA),

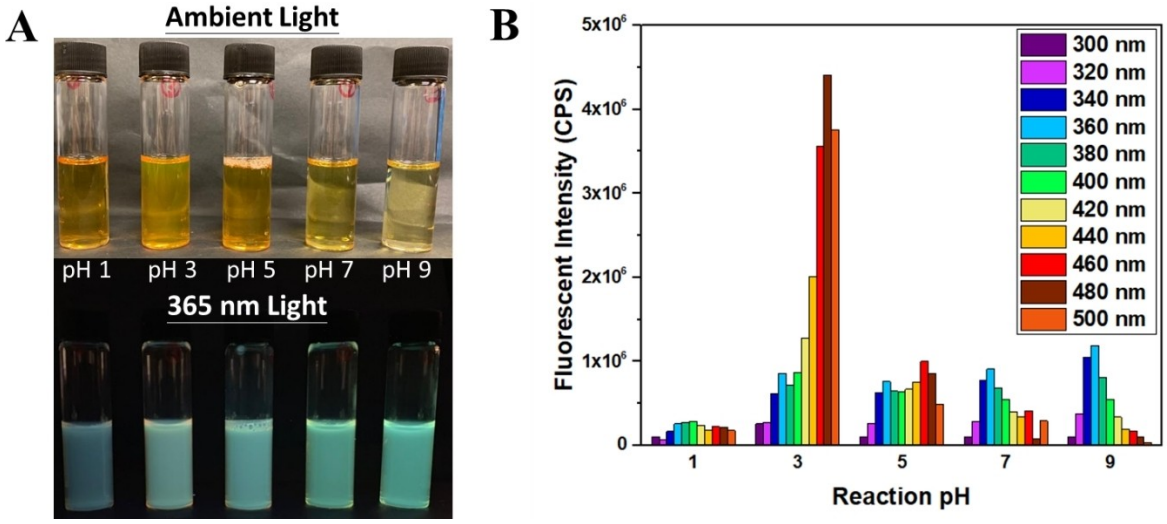

Figure 1. A) Images of gPEI/PMAA nanoparticles synthesized at pH 1, 3, 5, 7 and 9 under ambient light (top) and 365 nm light (bottom), B) The maximum fluorescence intensity of gPEI/PMAA nanoparticles synthesized at different pH values (1, 3, 5, 7, and 9).

methacrylic acid (MAA), and 2-carboxyethyl acrylate (CEA) were studied with different weight ratios between gPEI and the acrylic acid-based monomer (1:1, 1:2, 1:3, and 1:4) on particle size and size distribution. Polymerization was initiated with H_2O_2 at 80 °C and pH 3. The structural differences among the monomers can impact the formation of polyionic complexes with PEI, affecting the stability and properties of the resulting complexes. AA has a simple structure with minimal steric hindrance, allowing efficient interaction with PEI. MAA contains a methyl group, introducing steric hindrance and potentially reducing the accessibility of carboxylic acid groups for interaction with PEI. CEA has an extended side chain with an additional carboxylic group, which can increase steric hindrance but also provides more sites for interaction. The presence of additional groups, such as the methyl group in MAA and the extended chain in CEA can affect the flexibility and conformation of the polymer chains.

When MAA was polymerized, highly monodispersed nanoparticles were obtained at the gPEI to MAA weight ratios of 1:2 and 1:3 with average particle sizes of 35 and 47 nm, respectively (Figure S4). When CEA was polymerized, monomodal distribution of gPEI/PCEA nanoparticles was also obtained at the gPEI to CEA weight ratios of 1:2 and 1:3. However, the average particle sizes for these ratios were considerably larger, measuring at 178 nm and 258 nm, respectively, in comparison to the gPEI/PMAA nanoparticles (Figures S5). In the case of polymerization of AA with gPEI, multi-modal size distributions of gPEI/PAA nanoparticles were observed for all weight ratios (Figures S6). Based on these findings, it could be concluded that the polymerization of MAA in the presence of gPEI with a weight ratio of 2:1 would yield the smallest nanoparticles with a narrow particle size distribution.

Fluorescence intensities were measured and compared among the gPEI/PMAA, gPEI/PAA, and gPEI/PCEA nanoparticles with respect to their gPEI to monomer weight ratios (Figure 2 and Figures S7 and S8). The results indicated that gPEI/PMAA nanoparticles synthesized at the 1:2 weight ratio of gPEI to MAA exhibited the highest fluorescence intensity (Figure 2E). This suggests that the structural rigidity of the polymers plays a crucial role in polyionic complex formation and optical properties. Poly(methacrylic acid) (PMAA) possesses a more rigid structure than poly(acrylic acid) (PAA) due to the presence of a methyl group on the polymer backbone. This increased rigidity in PMAA leads to a greater restriction within the poly-ionic complexes formed in the nanoparticles, thus enhancing the fluorescence intensity. In contrast, poly(2-carboxyethyl acrylate) contains a flexible $–CH_2-CH_2-$ pendant group, creating more free volume within the polymer structure. This results in less restriction on the poly-ionic complexes, leading to weaker fluorescence intensity. Therefore, a polymer with higher backbone rigidity such as PMAA results in greater restriction on the motion of the polymer chains. This enhanced restriction facilitates stronger interactions between the sub-fluorophores (C–O, C–N, C=O, C=N) within the nanoparticles, leading to a more efficient radiative decay and consequently higher fluorescence intensity.

2.4. Properties of the gPEI/PMAA Nanoparticles

The chemical structures of native PEI, GA, gPEI, PMAA and gPEI/PMAA were analyzed using Fourier transform infrared (FTIR) spectroscopy (Figure S9). The characteristic peaks of PEI appeared at about 3400 cm^{-1} (N–H stretching), 1645 cm^{-1} (primary N–H bending), 1568 cm^{-1} (secondary N–H bending), 1470 cm^{-1} ($-CH_2-$ stretching) and 1312 cm^{-1} (C–N stretching). The spectrum of GA exhibited a peak at 1718 cm^{-1} representing C=O stretching. When comparing the spectrum of gPEI with the spectra of PEI and GA, the -NH_2 and -NH- peaks from PEI at 1645 cm^{-1} and 1560 cm^{-1} were still observed. The absorption at 1645 cm^{-1}, which corresponded to C=N group, increased, suggesting the formation of a Schiff's base as a result of the

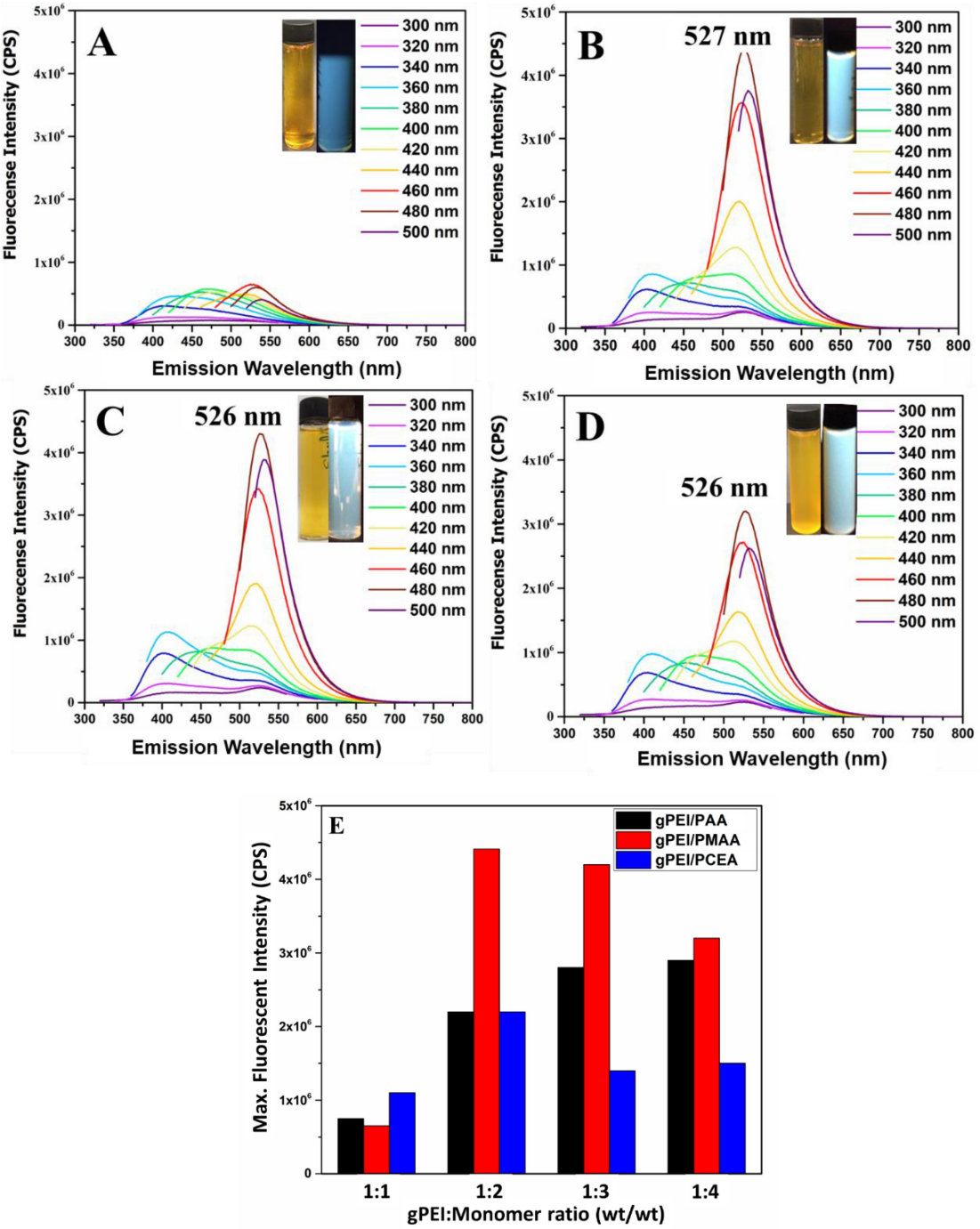

Figure 2. Fluorescence spectra of gPEI/PMAA nanoparticles synthesized with gPEI to MAA weight ratios of A) 1 : 1, B) 1 : 2, C 1 : 3, D) 1 : 4, and E) Comparison of fluorescence intensities of nanoparticles synthesized with MAA, AA and CEA at different gPEI to monomer weight ratios.

reaction between GA and the primary amine groups of PEI. After the polymerization of MAA, the gPEI/PMAA nanoparticles displayed a broad peak ranging from 2500–3500 cm^{-1}, which corresponded to O–H and N–H stretchings. A C=O stretching peak at 1700 cm^{-1} and a C–O stretching peak at 1172 cm^{-1} indicated the presence of PMAA polymer. The FTIR spectra confirmed the chemical composition of the nanoparticles, which contained glutaraldehyde-crosslinked PEI and PMAA polymer.

The morphology of the gPEI/PMAA nanoparticles, which were synthesized under optimal conditions (gPEI : MMA = 1 : 2 w/w, pH = 3, 3 h reaction), was examined using scanning electron microscopy (SEM). As shown in Figure 3B, the majority of the nanoparticles displayed a spherical shape with diameters ranging from 5 to 68 nm. The DLS measurement results indicated an average diameter of 35 nm for the nanoparticles with a PDI value of 0.29 (Figure 3A).

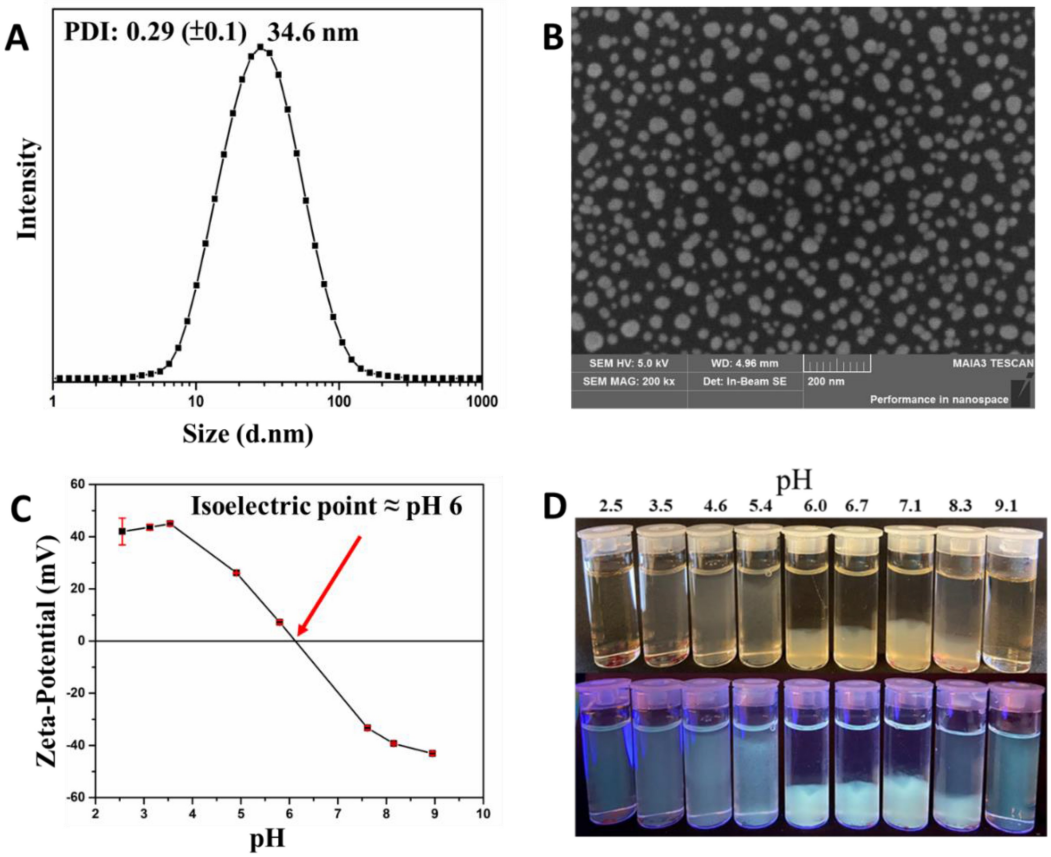

Figure 3. A) Particle size and size distribution of gPEI/PMAA nanoparticles; B) SEM image of gPEI/PMAA nanoparticles; C) *zeta*-Potential as a function of pH of gPEI/PMAA nanoparticles; and D) Images of gPEI/PMAA nanoparticles (1,000 ppm) at different solution pHs under ambient light (top) and 365 nm UV light (bottom). The gPEI/PMAA nanoparticles were synthesized with gPEI to MAA ratio of 1 : 2 (wt/wt) at pH 3.

The combining of gPEI and PMAA polymers through *in situ* copolymerization resulted in the formation of zwitterionic gPEI/PMAA complexed nanoparticles due to the presence of opposing charges. This zwitterionic nature of the nanoparticles is clearly demonstrated in Figure 3C, which depicts the *zeta*-potential as a function of pH. The isoelectric point of the gPEI/PMAA nanoparticles was found to occur at pH 6. It was observed that the nanoparticles became unstable around this pH value, resulting in aggregation of the nanoparticles as shown in Figure 3D. However, the nanoparticles exhibited stability at solution pH levels below 4 or above 9. This suggests that the gPEI/PMAA nanoparticles can maintain their dispersed state and stability in acidic or alkaline environments, while aggregation can occur at neutral pH conditions near the isoelectric point.

UV-Vis spectroscopy was used to analyze the absorption properties of native PEI, GA-modified PEI, and gPEI/PMAA nanoparticles. In the case of native PEI dissolved in water, only a very weak absorption signal between 250 and 320 nm was observed even at concentrations as high as 10 wt% (Figure 4A). After modifying PEI with GA, the resulting polymer exhibited a distinct absorption peak at 420 nm (Figure 4C). This absorption peak could be attributed to the formation of imine bonds, which were formed by the reaction between the primary amine groups of PEI and the aldehyde groups of GA. Figure 4E displays the gPEI/PMAA complexed nanoparticles which exhibit two absorption peaks at 326 and 475 nm. These peaks indicated that the nanoparticles possess distinct optical properties resulting from the formation of polyionic complexes.

Fluorescence spectroscopy was utilized to investigate the fluorescence properties of native PEI, GA-modified PEI, and gPEI/PMAA nanoparticles. The native PEI exhibited weak fluorescence even at concentration as high as 100,000 ppm with a maximum emission at 469 nm when excited by 360 nm light (Figure 4B). Notably, the fluorescence intensity of native PEI displayed dependence on the excitation wavelength. Upon crosslinking PEI with GA, the fluorescence intensity of PEI was significantly enhanced, and the color of the solution changed from colorless to pale yellow (Figure 4D). This observation was consistent with a previous study that suggested GA-modification altered the electronic structure of PEI, resulting in increasing fluorescence intensity.[47] The GA-modified PEI also exhibited excitation-dependent fluorescence characteristics. When excited by 400 nm light, the gPEI emitted maximum light intensity with a wavelength of 502 nm. This indicated that the modification of PEI with GA caused a red-shift in the maximum emission from 469 nm to 502 nm when they were excited at 360 nm and 400 nm, respectively. Figure 4F presents the fluorescence sprectra of gPEI/PMAA nanoparticles. These nanoparticles exhibited strong green fluorescence emissions in the

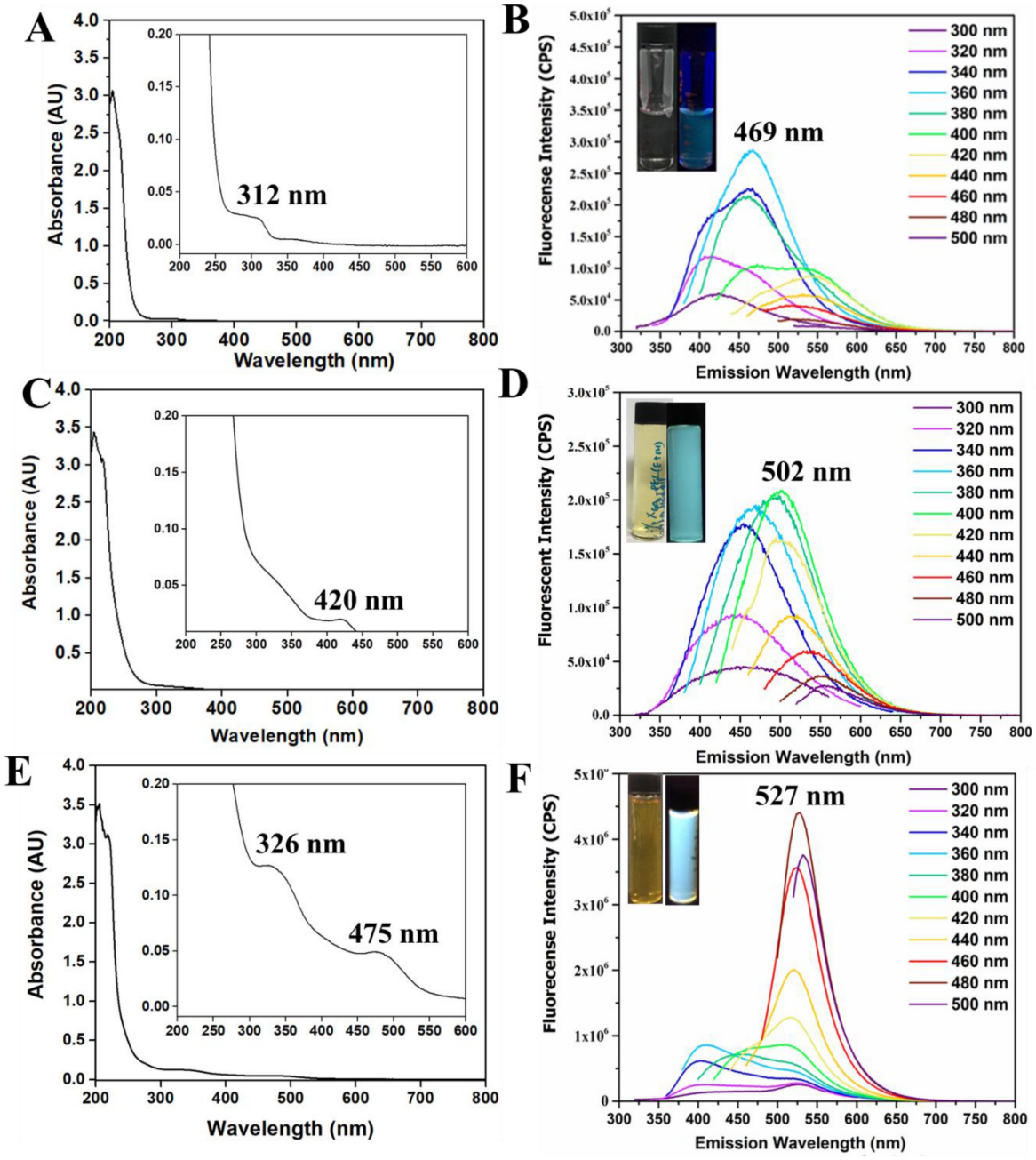

Figure 4. A and B) UV/Vis absorption and fluorescence spectra of 25 k PEI at a concentration of 100,000 ppm; C and D) UV/Vis absorption and fluorescence spectra of gPEI at a concentration of 1,000 ppm; E and F) UV/Vis absorption and fluorescence spectra of gPEI/PMAA nanoparticles at a concentration of 1,000 ppm.

range of 520 to 530 nm when excited at wavelengths of 460, 480, and 500 nm. Compared to gPEI, the excitation and emission maxima of gPEI/PMAA nanoparticles were further red-shifted to 480 nm and 527 nm, respectively. Furthermore, the maximum fluorescence intensity of the gPEI/PMAA nanoparticles was approximately ten times higher than that of gPEI as determined by fluorescence spectroscopy.

Non-traditional intrinsic luminescence is a novel emissive phenomenon occurring when typically non-emissive, electron-rich, hetero-atomic, sub-luminophoric moieties are arranged in specific molecular architectures, chemical cross-linked structures, or confined states. These configurations restrict intramolecular and intermolecular mobility, leading to unique emissive assemblies. Unlike traditional aromatic fluorophores, these materials usually exhibit blue-shifted fluorescence profiles (Ex. = 225–400 nm; Em. = 410–560 nm), primarily emitting in the blue region. A comprehensive review by Tomalia et al. summarizes the research progress and photoluminescent mechanisms of these non-conjugated PL materials.[48] Du et al. explored the synthesis of multicolored fluorescence in hyperbranched poly(amine ester), explaining their findings through theoretical calculations using the density functional theory (DFT)

method.[49] They proposed that dense clusters of NH, OH, and OC=O groups are crucial for the multicolored fluorescence observed in nonconventional luminogens. When these subunits are in close proximity, they readily form dense, strong inter/intrachain n-π* and π-π* interactions. These interactions, including dipole-dipole interactions like C=O···N–H and hydrogen bonding such as N–H···O, lead to electron cloud overlap, which further develops into an electronic delocalization system.

Based on these literature reports, we propose that the red-shifted photoluminescent properties of the poly-ionic complexes result from synergistic effects: 1) Charge transfer interactions: The formation of polyionic complexes between positively charged PEI and negatively charged PMAA facilitates charge transfer interactions, lowering the energy gap between ground and excited states, resulting in red-shifted emission. 2) Conjugation and planarization: Ionic interaction created compacted nanoparticles, thus enhancing conjugation or planarization of polymer chains. This extends electron delocalization, causing a red shift in photoluminescence. Further studies including experimental investigations and theoretical modeling of the electronic structure, molecular interactions, and energy states within the nanoparticle system, may reveal the exact mechanisms underlying this red-shift phenomenon.

The photoluminescence properties of the gPEI/PMAA nanoparticles were also characterized by measuring their relative quantum yield (QY) using quinine sulfate and Rhodamine 6G as reference standards (Figure S10 and S11). It was previously reported in the literature that native branched PEI exhibited a very low QY of less than 1%.[44] In our case, after modifying PEI with GA, the relative QY was increased to 5.39% (±0.38%). This indicated that the fluorescence intensity of the GA-modified gPEI was considerably enhanced compared to the native PEI. Furthermore, the relative QY of the gPEI/PMAA nanoparticles was further improved to 23.5% (±1.2%). This significant enhancement in the quantum yield demonstrated a substantial increase in the fluorescence intensity of the gPEI/PMAA nanoparticles compared to both native PEI and GA-modified gPEI.

The improved quantum yield and enhanced fluorescence properties of the gPEI/PMAA nanoparticles suggest that the incorporation of PMAA and the formation of nanoparticles play a crucial role. The incorporation of PMAA into the gPEI system introduces negatively charged segments that can electrostatically interact with the positively charged gPEI segments. This leads to the formation of poly-ionic complexed nanoparticles, where the gPEI and PMAA chains are intertwined and stabilized through electrostatic attractions. The formation of these poly-ionic complexes and the confinement within the nanoparticle structure can restrict the vibrational and rotational relaxation of the polymer chains. The confinement and close arrangement of sub-fluorophores in the nanoscale size can lead to a phenomenon known as through-space conjugation of chromophore cluster.[29] Through-space conjugation refers to the interaction of adjacent chromophores via non-covalent interactions without direct bonding. In the case of gPEI/PMAA nanoparticles, the sub-fluorophores, such as C–O, C–N, C=O, and C=N bonds, are confined within the nanoparticle structure and are in close proximity to one another. This close arrangement allows for efficient energy transfer between the sub-fluorophores, resulting in enhanced luminescence. Overall, the presence of heteroatomic bonds, the formation of poly-ionic complexes, and the confinement of sub-fluorophores within the nanoscale dimensions of gPEI/PMAA nanoparticles contribute to the through-space conjugation of chromophore cluster, enabling efficient energy transfer and enhancing the photoluminescence properties of the nanoparticles.

2.5. gPEI/PMAA Nanoparticles as Phosphors for WLEDs

One approach to creating a white light emitting diode (LED) chip involves the integration of blue and green light sources to achieve the desired color temperature. In this study, we investigated the potential of gPEI/PMAA nanoparticles, which emitted green light at a wavelength of 528 nm, to generate a white LED when combined with a monochromatic blue light source. This method offered the advantage of simplifying the design of LED lighting systems by combining the blue light emitted by the LED chip with the green light emitted by the nanoparticles embedded in the silicon enclosure.

Figure 5 and Table S1 show the optical properties of LED chips coated with silicon containg different weight percentages (10, 20 and 30 wt%) of nanoparticles. The correlated color temperatures (CCT), which is a specification of the color appearance of the light emitted by a light source, were deterimined. The CCT values of the LED coated with 10 and 20 wt% nanoparticles were within the range of warm white to natural white light at 3648 and 5269 K, respectively. However, the CCT value of 30 wt% nanoparticles coated LED was 1877 K, which was out of the light range. Moreover, the D_{uv} values of these coated LEDs were all less than 0.02. This indicated that the light emitted by the LEDs was within the white region of the CIE 1931 XYZ color space as defined by the International Commission on Illumination. Additionally, the color rendering index (CRI) values for white LEDs containing 10% and 20% of gPEI/PMAA nanoparticles were above 80 Ra. This implied that these LEDs could be classified as good chips in terms of color rendering quality.[50]

The use of gPEI/PMAA nanoparticles for white LED production offers several advantages: 1) Tunable color properties: gPEI/PMAA nanoparticles allow for the production of white LEDs with desirable and adjustable colors. By varying the weight percentage, the CCT and CRI of the LEDs can be tailored to specific requirements. This flexibility in color control is advantageous for various lighting applications where specific color temperatures or color rendering characteristics are desired. 2) Simplified design: The integration of gPEI/PMAA nanoparticles as a green light source activated by a monochromatic blue light simplifies the design of LED lighting systems. The combination of blue light emitted by the LED chip with the green light emitted by the nanoparticles eliminates the need for complex color mixing mechanisms or multiple light sources. This simplification can lead to cost savings and easier manufacturing processes. 3) Compatibility with silicone enclosure: The gPEI/PMAA nanoparticles can be embedded

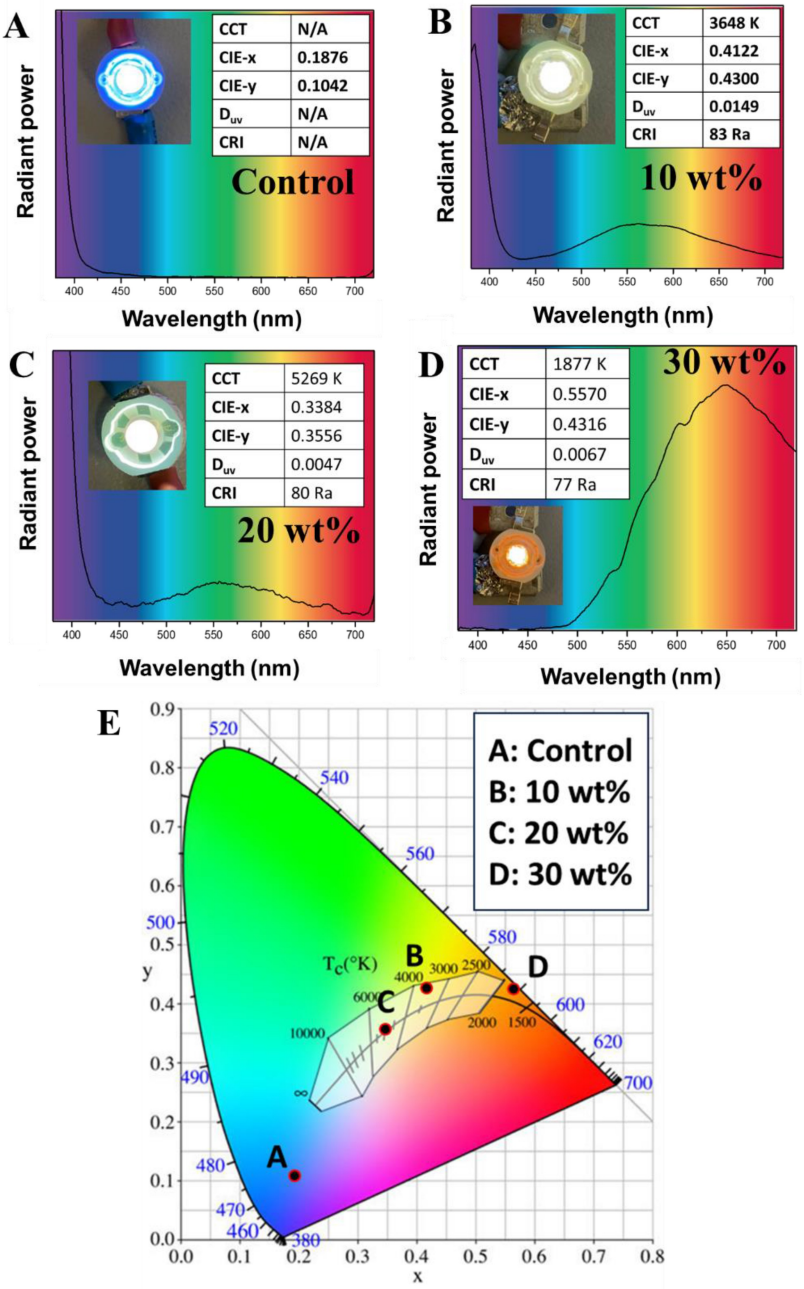

Figure 5. Light spectrum, CCT, CIE, D_{uv} and CRI of LED uncoated and coated with gPEI/PMAA nanoparticles: A) 0 wt% (Control); B) 10 wt%; C) 20 wt% and D) 30 wt%. E) CIE_{xy} 1931 chromaticity diagram with Planckian locus and lines of correlated color temperature of LED chips coated with A) 0 wt% (Control); B) 10 wt%; C) 20 wt% and D) 30 wt% of gPEI/PMAA nanoparticles.

within a silicone enclosure, which is a common material used in LED fabrication. This compatibility ensures good adhesion and stability of the nanoparticles within the LED structure, enhancing the performance and longevity of the white LED. These advantages make green fluorescence gPEI/PMAA nanoparticles a promising material for white LED production, offering versatility, simplified design, and high-quality light output.

3. Conclusions

We have developed a methodology for synthesizing non-conjugated green fluorescence nanoparticles in an aqueous medium. The synthesis process involves two main steps: crosslinking polyethyleneimine with glutaraldehyde in ethanol and subsequent *in situ* polymerization of an acrylic acid-based monomer. The combination of the crosslinked PEI and the polymerized acrylic acid-based monomer results in the formation of poly-ionic complexed nanoparticles. The SEM analysis has revealed the spherical morphology of the gPEI/PMAA

nanoparticles, and the *zeta*-potential measurements have provided insights into their zwitterionic characteristics and pH-dependent stability. The glutaraldehyde-crosslinked PEI/poly(methacrylic acid) (gPEI/PMAA) nanoparticles have exhibited robust green fluorescence emissions within the range of 520 to 530 nm when excited by wavelengths of 460, 480, and 500 nm with a high quantum yield up to 23.5%. This green fluorescence capability has been effectively utilized as a green light source in the fabrication of LEDs. The non-conjugated gPEI/PMAA nanoparticles with their distinctive green fluorescence characteristics offer potential for diverse applications including light-emitting diodes, optoelectronic devices, bioimaging, and fluorescence-based sensing systems.

Experimental Sections

Materials

Branched polyethyleneimine [PEI, number average molecular weight (M_n) ≈10 kDa, weight average molecular weight (M_w) ≈25 kDa] and glutaraldehyde (GA, 50 wt% in H_2O) were obtained from Sigma Aldrich and used as received. Methacrylic acid (MAA), acrylic acid (AA), and 2-carboxyethyl acrylate (CEA) were also obtained from Sigma Aldrich and purified using a column packed with inhibitor removers (Sigma Aldrich). Hydrogen peroxide (H_2O_2, 35 wt% in water, Riedel-de Haën) was diluted to a concentration of 100 mM with Milli-Q water and stored at 4 °C. Cellulose dialysis tubing with a molecular weight cut-off of 12,400 Da (Sigma Aldrich) was used for purification. Absolute ethanol (GR Grade) was obtained from DUKS. Milli-Q water (H_2O) was used as the dispersion medium. Organic silicon (ZWL8820, containing components A and B) was purchased from Shenzhen Looking Long Technology Co., LTD (China).

Synthesis of Crosslinked Polyethyleneimine with Glutaraldehyde (gPEI)

In a typical batch of 200 g, a mixture of 10 g of branched polyethyleneimine (PEI) dissolved in 90 g of ethanol (EtOH) was mixed with 100 g of EtOH solution containing 0.945 g of glutaraldehyde (GA, 50 wt% in H_2O) through a dropwise addition. The mixture was stirred at room temperature for 24 hours. The color of the resulting solution changed from clear to pale yellow. The mixture was subsequently mixed with 200 g water and the EtOH was removed via a rotary evaporator. The aqueous solution was then subjected to purification by dialysis against Milli-Q water until the conductivity of the dialysate fell below the threshold of 30 μS/cm.

Synthesis of Poly-Ionic Complexed Nanoparticles

The prepared solution of glutaraldehyde crosslinked polyethyleneimine (gPEI), which had a total weight of 42.39 g and a concentration of 2.36 wt%, was mixed with purified monomer (ranging from 1 to 4 g). The pH of the mixture was then adjusted using either 2 M HCl or 2 M NaOH to pH values of 1, 3, 5, 7 or 9 and diluted with water to final weight of 99 g. The resulting mixture was transferred to a double-layered flask reactor equipped with a magnetic stirrer, a nitrogen inlet, a thermometer, and a condenser. The mixture was stirred under nitrogen at a rate of 450 rpm for 10 minutes at room temperature, followed by heating to 80 °C. The polymerization was initiated by adding 1 mL of 100 mM H_2O_2, and the reaction was allowed to carry on for 3 hours. The solution changed from a clear pale-yellow solution to a brown turbid dispersion during the reaction. The crude product was subsequently purified through dialysis against Milli-Q water until the conductivity of the dialysate fell below 30 μS/cm.

Measurement and Characterization

The fourier transform infrared (FTIR) spectrum was recorded on a Nicolet iS50 FT-IR spectrometer using a KBr disk over the spectral range of 500–4000 cm^{-1}. The particle size and size distribution were determined by dynamic light scattering (DLS) using a Malvern Zetasizer Nano ZS equipped with a photon correlation spectroscopy, electrophoretic dynamic light scattering as well as a two-laser diode light source with a wavelength of 632.8 nm at 4 mW, and operated at a detector angle of 173°. For particle size measurement, samples were diluted to 1000 ppm in aqueous solution, and for *zeta*-potential measurement, samples were diluted to 1000 ppm in a 1 mM NaCl solution. Results of the particle size and *zeta*-potential were obtained as an average of triplicate measurements. The morphology of the nanoparticles was examined using a field-emission scanning electron microscope (FE-SEM, TESCAN MAIA3). The sample was dried on a P-type silicon chip substrate (SPI, 4136SC-AB), then coated it with a thin layer of gold using an ion sputter coater (SEC, MCM-200). The UV-visible spectrum was obtained using an UV-Vis spectrometer (Agilent Technology Cary 8454), covering a range from 200 to 800 nm. The sample was diluted to a concentration of 1000 ppm with Milli-Q water prior to measurement. The fluorescence spectrum was obtained using a spectrofluorometer (Horiba FluoroMax-4), with excitation wavelengths ranging from 300 to 500 nm and a fixed increment of 20 nm.

The quantum yields (QYs) of the gPEI and gPEI/PMAA nanoparticles were determined using the relative quantum yield method. Quinine sulfate and rhodamine 6G were chosen as reference standards, with excitation wavelengths of 360 and 480 nm, respectively. At least five sample solutions or dispersions were prepared by dilution with Milli-Q water to achieve absorbances ranging from 0.01 to 0.1 a.u. at the respective excitation wavelengths. Quinine sulfate and rhodamine 6G were diluted in 0.5 M H_2SO_4 solution and absolute ethanol, respectively, to obtain absorbances ranging from 0.01 to 0.1 a.u. at their respective excitation wavelengths. The fluorescence emission spectra of the as-prepared solutions or dispersions were measured by the spectrofluorometer. The quantum yield of the samples, QY_x, was then calculated by the Equation (1):

$$QY_x = QY_s \times \frac{A_s}{A_x} \times \frac{F_x}{F_s} \times \frac{n_x^2}{n_s^2} = QY_s \times \frac{m_x}{m_s} \times \frac{n_x^2}{n_s^2} \quad (1)$$

where QY_s is the quantum yield of the standard, A_x and A_s are the absorbances of the sample and standard, respectively, F_x and F_s are the integrated fluorescence intensities of the sample and standard, respectively, n_x and n_s are the reflective indexes of the sample and standard, respectively, and m_x and m_s are the slopes of integrated fluorescence intensity vs absorbance plot of the sample and standard, respectively (Figure S10 and S11).

Fabrication of White Light Emitting Diodes (WLEDs)

The dry powder of gPEI/PMAA nanoparticles was prepared using a vacuum freeze dryer (LABFREEZ, FD-10-R). Different quantities of nanoparticles (10, 20 and 30 wt% to total silicone) were mixed thoroughly with silicone component B, followed by mixing with silicone component A at room temperature. The mixing ratio of

component A to component B was in accordance with the supplier's recommendation of 1 : 4 (wt/wt). The resulting mixture was degassed under vacuum at room temperature for 30 minutes, after which 5 mg mixture was coated onto 365 nm LED chips. The samples were subsequently cured at 60 °C for 40 minutes, followed by heating at 135 °C for 110 minutes in an oven.

The coated LED chips were connected to a power supply (Major Science MP-250 N) with a 120 mA current, and the correlated color temperature (CCT), color rendering index (CRI), and deep ultraviolet (Duv) were measured using a light detector (AsenseTek Lighting passport, ALP-01, Taiwan).

Acknowledgements

The authors gratefully acknowledge the financial support from the Hong Kong Polytechnic University and Hong Kong Special Administrative Regions (HKSAR) Innovation and Technology Fund (ITS/016/18).

Conflict of Interests

The authors declare no conflict of interest.

Data Availability Statement

The data that support the findings of this study are available from the corresponding author upon reasonable request.

Keywords: Green fluorescence · Non-conjugated polymer · Crosslinking · Polyethyleneimine · Poly-ionic complexes · Nanoparticles

[1] M. Clark, *Handbook of Textile and Industrial Dyeing*, Woodhead Publishing, Philadelphia, PA, **2011**.
[2] L. Ying, C. L. Ho, H. Wu, Y. Cao, W. Y. Wong, *Adv. Mater.* **2014**, *26*, 2459.
[3] N. C. Shaner, P. A. Steinbach, R. Y. Tsien, *Nat. Methods.* **2005**, *2*, 905.
[4] H. Tazawa, K. Shigeyasu, K. Noma, S. Kagawa, F. Sakurai, H. Mizuguchi, H. Kobayashi, T. Imamura, T. Fujiwara, *Cancer Sci.* **2022**, *113*, 1919.
[5] K. Baatout, F. Saad, A. Baffoun, B. Mahltig, D. Kreher, N. Jaballah, M. Majdoub, *Mater. Chem. Phys.* **2019**, *234*, 304.
[6] Z. He, S. Shen, G. Zhang, T. Miao, X. Cheng, Z. Wang, Q. Song, W. Zhang, *Aggregate* **2023**, *4*, e351.
[7] J. Qi, X. Hu, X. Dong, Y. Lu, H. Lu, W. Zhao, W. Wu, *Adv. Drug Deliv. Rev.* **2019**, *143*, 206.
[8] R. Xu, P. Zhang, Q. Shen, Y. Zhou, Z. Wang, Y. Xu, L. Meng, D. Dang, B. Zhong Tang, *Coord. Chem. Rev.* **2023**, *477*, 214944.
[9] H. Nie, K. Hu, Y. Cai, Q. Peng, Z. Zhao, R. Hu, J. Chen, S. J. Su, A. Qin, B. Z. Tang, *Mater. Chem. Front.* **2017**, *1*, 1125.
[10] R. Hu, N. L. C. Leung, B. Z. Tang, *Chem. Soc. Rev.* **2014**, *43*, 4494.
[11] Y. Y. Chen, S. C. Fan, C. C. Chang, J. C. Wang, H. M. Chiang, T. Y. Juang, *ACS Omega* **2021**, *6*, 33159.
[12] C. H. Li, W. F. Wang, N. Stanislas, J. L. Yang, *RSC Adv.* **2022**, *12*, 7911.
[13] Y. Sun, W. Cao, S. Li, S. Jin, K. Hu, L. Hu, Y. Huang, X. Gao, Y. Wu, X. J. Liang, *Sci. Rep.* **2013**, *3*, 3036.
[14] D. S. Bhattacharya, A. Bapat, D. Svechkarev, A. M. Mohs, *ACS Omega* **2021**, *6*, 17890.
[15] Z. A. Qiao, Q. Huo, M. Chi, G. M. Veith, A. J. Binder, S. Dai, *Adv. Mater.* **2012**, *24*, 6017.
[16] D. Tong, W. Li, Y. Zhao, L. Zhang, J. Zheng, T. Cai, S. Liu, *RSC Adv.* **2016**, *6*, 97137.
[17] Y. Chen, Y. Zhang, T. Lyu, Y. Wang, X. Yang, X. Wu, *J. Mater. Chem. C.* **2019**, *7*, 9241.
[18] Z. Zhong, L. Jia, *Talanta* **2019**, *197*, 584.
[19] J. Liu, F. Wu, A. Xie, C. Liu, H. Bao, *Anal. Bioanal. Chem.* **2020**, *412*, 1235.
[20] Y. Tang, X. Zhou, K. Xu, X. Dong, *Spectrochim. Acta A Mol. Biomol. Spectrosc.* **2020**, *240*, 118626.
[21] S. Liu, H. Liu, Q. Chen, J. Hou, G. Yang, *Microchim. Acta.* **2021**, *189*, 36.
[22] J. Liu, T. Fu, C. Liu, F. Wu, H. Wang, *Nanotechnology* **2021**, *32*, 355503.
[23] B. Han, Q. Yan, Q. Liu, D. Li, Y. Chen, G. He, *Sep. Purif. Technol.* **2022**, *292*, 121023.
[24] S. G. Liu, T. Liu, N. Li, S. Geng, J. L. Lei, N. B. Li, H. Q. Luo, *J. Phys. Chem. C.* **2017**, *121*, 6874.
[25] S. Zhu, L. Wang, N. Zhou, X. Zhao, Y. Song, S. Maharjan, J. Zhang, L. Lu, H. Wang, B. Yang, *Chem.Commun.* **2014**, *50*, 13845.
[26] S. Zhu, Y. Song, J. Shao, X. Zhao, B. Yang, *Chem. Commun.* **2015**, *54*, 14626.
[27] S. Tao, S. Zhu, T. Feng, C. Zheng, B. Yang, *Angew. Chem.* **2020**, *132*, 9910.
[28] X. Dou, Q. Zhou, X. Chen, Y. Tan, X. He, P. Lu, K. Sui, B. Z. Tang, Y. Zhang, W. Z. Yuan, *Biomacromolecules* **2018**, *19*, 2014.
[29] P. Liao, J. Huang, Y. Yan, B. Z. Tang, *Mater. Chem. Front.* **2021**, *5*, 6693.
[30] J. Liu, H. Bao, C. Liu, F. Wu, F. Gao, *ACS Appl. Polym. Mater.* **2019**, *1*, 3057.
[31] H. Liu, R. S. Li, J. Zhou, C. Z. Huang, *Analyst* **2017**, *142*, 4221.
[32] C. Wang, Z. Xu, C. Zhang, *ChemNanoMat* **2015**, *1*, 122.
[33] J. Li, L. Zheng, H. Cai, W. Sun, M. Shen, G. Zhang, X. Shi, *Biomaterials* **2013**, *34*, 8382.
[34] Y. Jia, D. Niu, Q. Li, H. Huang, X. Li, K. Li, L. Li, C. Zhang, H. Zheng, Z. Zhu, X. Zhao, P. Li, G. Yang, *Nanoscale.* **2019**, *11*, 2008.
[35] X. Wang, D. Niu, C. Hu, P. Li, *Curr. Pharm. Des.* **2015**, *21*, 6140.
[36] Y. S. Siu, L. Li, M. F. Leung, K. L. D. Lee, P. Li, *Biointerphases* **2012**, *7*, 16.
[37] J. Zhu, A. Tang, L. P. Law, M. Feng, K. M. Ho, D. K. L. Lee, F. W. Harris, P. Li, *Bioconjugate Chem.* **2005**, *16*, 139.
[38] M. Feng, P. Li, *J. Biomed. Mater. Res.* **2007**, *80 A*, 184.
[39] Z. Géczi, P. Hermann, L. Kőhidai, O. Láng, Z. Kőhidai, T. Mészáros, A. Barócsi, S. Lenk, T. Zelles, *J. Nanomater.* **2018**, *2018*, 1048734.
[40] S. Azlin-Hasim, M. C. Cruz-Romero, E. Cummins, J. P. Kerry, M. A. Morris, *J. Colloid Interface Sci.* **2016**, *461*, 239.
[41] Z. M. Ayalew, X. Guo, X. Zhang, *J. Hazard. Mater. Adv.* **2022**, *8*, 100158.
[42] T. C. Drage, K. M. Smith, A. Arenillas, C. E. Snape, *Energy Procedia* **2009**, *1*, 875.
[43] H. Kassab, M. Maksoud, S. Aguado, M. Pera-Titus, B. Albela, L. Bonneviot, *RSC Adv.* **2012**, *2*, 2508.
[44] L. Pastor-Pérez, Y. Chen, Z. Shen, A. Lahoz, S. E. Stiriba, *Macromol. Rapid Commun.* **2007**, *28*, 1404.
[45] K. M. Ho, W. Y. Li, C. H. Lee, C. H. Yam, R. G. Gilbert, P. Li, *Polymer* **2010**, *51*, 3512.
[46] I. Insua, A. Wilkinson, F. Fernandez-Trillo, *Eur. Polym. J.* **2016**, *81*, 198.
[47] Y. Ling, F. Qu, Q. Zhou, T. Li, Z. F. Gao, J. L. Lei, N. B. Li, H. Q. Luo, *Anal. Chem.* **2015**, *87*, 8679.
[48] D. A. Tomalia, B. Klajnert-Maculewiczd, K. A.-M. Johnsonc, H. F. Brinkmanc, A. Janaszewskad, D. M. Hedstrand, *Prog. Polym. Sci.* **2019**, *90*, 35.
[49] Y. Du, T. Bai, H. Yan, Y. Zhao, W. Feng, W. Li, *Polymer* **2019**, *185*, 121771.
[50] W. D. van Driel, X. J. Fan, *Solid State Lighting Reliability: Components to Systems*, Springer New York, NY **2013**.

Manuscript received: April 29, 2024
Revised manuscript received: October 21, 2024
Accepted manuscript online: November 1, 2024
Version of record online: November 28, 2024